




Article

Effects of polypropylene glycol-treated montmorillonite/carbon black as a filler with rubber compound properties

Zohreh Asghari Barzegar and Mercedeh Malekzadeh 

Chemistry Department, North Tehran Branch, Islamic Azad University, Tehran, Iran

Abstract

Carbon black is commonly used as a filler in the rubber industry. However, it can cause serious damage to human health and to ecosystems. Today, reducing the use of this substance *via* alternative materials is receiving increased attention. Clay minerals such as montmorillonite can be substituted for carbon black as environmentally friendly fillers for rubber compounds. The uniform dispersion of montmorillonite and its compatibility with the rubber matrix are the main principles for using this material in the rubber industry. To this end, montmorillonite was surface treated with various dosages (1.0, 1.5 and 2.0 wt.%) of polypropylene glycol. The surface-treated montmorillonites were investigated using attenuated total reflection Fourier-transform infrared spectroscopy, thermogravimetric analysis, scanning electron microscopy and X-ray diffraction analysis. The results indicated that the treatment expanded the interlayer spaces of the montmorillonite and improved surface hydrophobicity. The untreated and treated montmorillonites were used with carbon black as dual fillers in natural rubber/styrene butadiene-based compounds. The cure characteristics, thermal stability, some mechanical properties and dispersion states were evaluated. The curing study indicated a faster optimum cure time, scorch time and increased torque difference for the rubber compounds filled with surface-treated montmorillonites. Thermal analysis of the rubber compounds illustrated that the interval between the initial and final temperature of decomposition could be increased *via* the treatment. Surface-treated montmorillonite samples, especially the sample containing 1 wt.% polypropylene glycol, showed improved abrasion resistance, resilience and compression set values.

Keywords: Cure characteristics; mechanical properties; montmorillonite; polypropylene glycol; rubber; surface treatment; thermal properties

(Received: 11 July 2024; revised: 11 September 2024; Associate Editor: Chun-Hui Zhou)

Rubbers can be applied in several products, such as in tyres, tubes and airbags, among others (Zhang *et al.*, 2019; Kazemi *et al.*, 2022). However, most rubbers in their raw state have poor mechanical and thermal properties, so they need to be reinforced (Wang *et al.*, 2019; Sarma *et al.*, 2021; Kazemi *et al.*, 2022). A simple, popular and economical method to improve the mechanical properties of rubber compounds is using fillers (Zhang *et al.*, 2012; Alwis *et al.*, 2020). Fillers are also added to rubber compounds to decrease the costs of and facilitate their production (Arroyo *et al.*, 2003). Common fillers include carbon black, calcium carbonate, clay minerals, silica and calcium silicate (Moonchai *et al.*, 2012). Among these, carbon black is widely used as a reinforcing filler in the rubber industry due to its ability to improve the mechanical properties of rubber compounds (Seo *et al.*, 2018; Alwis *et al.*, 2020; Utrera-Barrios *et al.*, 2021). However, carbon black derives from petroleum, the use of which can cause environmental pollution and the emission of greenhouse gases (Seo *et al.*, 2018; Kazemi *et al.*, 2022). These drawbacks have increased interest in using environmentally friendly fillers such as clay minerals (Moonchai *et al.*, 2012; Pajtášová *et al.*, 2017; Alwis *et al.*, 2020).

Montmorillonite (Mnt) is an essential clay mineral (Liu *et al.*, 2019; Wójcik-Bania *et al.*, 2021) belonging to the smectite group that is a member of 2:1 phyllosilicate family (Archibong *et al.*, 2023; Safarik & Prochazkova, 2024). Mnt is a layered crystalline material, consisting of two tetrahedral sheets of silica with an octahedral sheet of alumina (Miedzianowska *et al.*, 2021; Archibong *et al.*, 2023). The octahedral sheet is sandwiched between the two tetrahedral sheets. The Mnt layer thickness is ~ 1 nm along the regular space in its interlayer space (Chrissafis & Bikiaris, 2011; Liu *et al.*, 2019; Madejova *et al.*, 2023); the lateral dimensions of the layers are between 30 nm and several microns or larger (Chrissafis & Bikiaris, 2011). The molecular formula of Mnt is $M_x(\text{Al}_{4-x}\text{Mg}_x)\text{Si}_8\text{O}_{20}(\text{OH})_4$, where M is a monovalent cation (Krol-Morkisz & Pielichowska, 2018; Olszewski *et al.*, 2023). The aluminium ions (Al^{3+}) can be partially replaced with divalent magnesium cations (Mg^{2+}) in the octahedral sheet, and the Si^{4+} can be replaced with Al^{3+} in the tetrahedral sheet. In these situations, negative charges are created and distributed in the platelets. These charges can be counterbalanced by positive ions such as Ca^{2+} and Na^+ (Chen *et al.*, 2023; Kovalchuk, 2023; Su *et al.*, 2023). The monovalent interlayer cations of Mnt cause the swelling of this substance due to water absorption in the interlayer space (Krzaczkowska *et al.*, 2005; Yotsuji *et al.*, 2021; Christidis *et al.*, 2023).

Corresponding author: Mercedeh Malekzadeh; Email: m_malekzadeh@iau-tnb.ac.ir

Cite this article: Asghari Barzegar Z and Malekzadeh M (2024) Effects of polypropylene glycol-treated montmorillonite/carbon black as a filler with rubber compound properties. *Clay Minerals* 59, 287–297. <https://doi.org/10.1180/clm.2024.26>

© The Author(s), 2025. Published by Cambridge University Press on behalf of The Mineralogical Society of the United Kingdom and Ireland.

Mnt can be used as a reinforcing filler in rubber compounds (Fathurrohman *et al.*, 2020; Archibong *et al.*, 2023). Specific properties of rubber compound such as their flame retardancy and barrier properties can be improved by using fillers such as these (Ahmadi *et al.*, 2022; Zhou *et al.*, 2022; Antosik *et al.*, 2023). In addition, particles of Mnt have a greater surface area than other fillers, thereby reducing the amount of filler that is needed to fill such rubber compounds (Lan *et al.*, 2012). However, the charged nature of Mnt can produce hydrophilic surfaces, leading to incompatibility of Mnt with hydrophobic polymers (Das *et al.*, 2011; Miedzianowska *et al.*, 2021). Hence, to overcome this problem and gain compatibility and uniform dispersion without agglomeration in the polymer matrix, the surface treatment of Mnt is essential (Krol-Morkisz & Pielichowska, 2018; Gua *et al.*, 2020; Wójcik-Bania *et al.*, 2021). Various methods have been used for the treatment of Mnt. Radiation (Mohamed *et al.*, 2013), cation-exchange reactions (Xi *et al.*, 2007; Jincheng *et al.*, 2013), using corrosive microorganisms (Meng *et al.*, 2022) and applying organic modifiers are the most important such approaches. Today, particular attention is being paid to the use of organic modifiers. Various materials have been used for this purpose, such as surfactants (Zhou *et al.*, 2009; Wójcik-Bania *et al.*, 2021; Yu *et al.*, 2021; Arabmofrad *et al.*, 2023), salts of octadecanoic acid and dodecanoic acid (Sarier & Onder, 2010), octadecylamine (Pattamaprom & Jiamjitsiripong, 2012), amines (Rath *et al.*, 2012), latex (Al-Shemmari *et al.*, 2013), silane derivatives (Song & Sandi, 2001; Bertuoli *et al.*, 2014; Shuai *et al.*, 2020; Baghitabar *et al.*, 2023), gum rosin (Esmaeili *et al.*, 2021), diphenylmethane diisocyanate (Krol-Morkisz & Pielichowska, 2018) and polyethylenimine and poly-2-methyl-2-oxazoline (Madejova *et al.*, 2023), among others. Industrial use of this method may be limited due to the toxicity of these organic modifiers (Moustafa *et al.*, 2020).

Today, research is moving towards the use of more accessible and easy-to-use organic modifiers. Polypropylene glycol (PPG) is a cheap and non-corrosive material with lubricating and freeze-protection effects. It is also compatible with rubber matrices. In this work, the surface treatment of Mnt by PPG was considered using various PPG dosages. The obtained surface-treated Mnt (St-Mnt) samples were applied as dual fillers with carbon black in a natural rubber (NR)/styrene butadiene rubber (SBR) compound. Using such a dual filler can reduce carbon black consumption in rubber compounds, thereby decreasing its harmful environmental effects. The cure characteristics, mechanical properties and thermal stability of the compounds were investigated and compared to rubber compounds filled with Mnt/carbon black. This new approach has not been received sufficient attention to date, and this work aims to fill this gap in the research.

Experimental

Materials

Mnt was obtained from Sigma-Aldrich (Steinheim, Germany). PPG (Mw = 2000) and ethanol (99%) were purchased from Merck (Darmstadt, Germany). Standard Malaysian rubber (SMR) 20 as the NR sample was supplied from The Ah Yau Rubber Factory (Bedong, Malaysia). SBR 1500 (23% styrene) was supplied by Bandar Imam Petrochemical (Mahshahr, Iran). Sulfur (purity $\geq 99.7\%$) was obtained from Tesdak (Saveh, Iran). Aromatic oil (No. 290) was purchased from Behran Oil (Tehran, Iran). 2,2,4-Trimethyl-1,2-di-hydroquinoline (TMQ) was provided by Rongcheng (Rongcheng, China). Carbon black N-330 was

supplied by Iran Carbon (Ahvaz, Iran). Antilux 654 was provided from Rhein Chimie (Mannheim, Germany). N-cyclohexyl-2-benzothiazole sulfenamide (CBS; purity $\geq 98.5\%$) was supplied by Taizhou Chemical (Taizhou, China). Zinc oxide (purity $\geq 99.0\%$) was obtained from Shokohie (Qom, Iran). Stearic acid (purity $\geq 95\%$) was obtained from Palmoleo Sdn. Bhd. (Selangor, Malaysia). N-(1,3-dimethylbutyl)-N'-phenyl-p-phenylenediamine (6PPD; active substance $\geq 97\%$) was supplied by Duslo (Šal'a, Slovakia).

Methods

Attenuated total reflection Fourier-transform infrared (ATR-FTIR) spectroscopy was carried out using a FTIR spectrometer with ATR cells from Bruker (Ettlingen, Germany). Thermogravimetric analysis (TGA) was performed using TA 1500 from Scinco (Seoul, Korea); heating of the samples was carried out under an inert atmosphere (nitrogen) from ambient temperature up to 900°C at a heating rate of 20°C min⁻¹ (for rubber compounds, after ~550°C the nitrogen atmosphere was changed to an air atmosphere, then heating was continued to obtain a constant mass loss). Scanning electron microscopy (SEM) analysis was conducted using a Yegaiitecan Analyzer (Fuveau, France); the samples were coated with a thin gold layer before the SEM analyses. X-ray diffraction (XRD) analysis was performed using a Philips X'Pert MPD device (Eindhoven, The Netherlands) with a Cu-K α radiation source at a wavelength of 0.154056 nm, operating at voltage of 40 kV and with current values of 30 mA. The scanning step rate was 0.02° s⁻¹ and the 2 θ angle range was between 1° and 10°. Measurement of the cure properties was performed at 160°C according to ASTM D 5289 using an MDR 900 rheometer from Hiwa (Tehran, Iran). The curing of the rubber compounds for making tablets and sheets was performed at 160°C using hot press moulds. The abrasion resistance of the samples was measured using an Abrasion Tester device from Bareiss (Oberdisingen, Germany) according to ASTM D 5963. The compression set measurements were obtained according to ASTM D 395(B) using a Gotech device (Taichung, Taiwan). Rebound resilience was assessed using a Rebound Tester device from HIWA (Tehran, Iran) according to ASTM D 7121. Ozone resistance was performed using equipment from Shandong Drick Instruments (Jinan, China) according to ASTM D 1149. These properties were measured for five specimens and the median values are reported.

Surface treatment of Mnt by PPG

A total of 30 g Mnt was dispersed in 37.5 mL water. The preparation of St-Mnt with 1 wt.% PPG was performed by dissolving 0.3 mL PPG in 3.75 mL ethanol and adding it to the aqueous suspension of Mnt. After that, the obtained mixture was agitated in an ultrasonic bath for 15 min, stirred for 2 h at 40°C and filtered. The obtained particles were washed with distilled water and then dried for 6 h at 80°C. The same procedure was performed for the preparation of the 1.5 wt.% and 2.0 wt.% PPG loadings using 0.45 and 0.60 mL PPG, respectively.

Compound recipe

For preparation of the rubber compounds, the compound ingredients were put in a two-roll mill (SYM-8, Wellshayang, 8" \times 20";

Table 1. Compound formulation process.

Component (phr)	Compound no.			
	1	2	3	4
SMR 20 (NR)	75	75	75	75
SBR	25	25	25	25
Carbon black N-330	35	35	35	35
Aromatic oil	10	10	10	10
Zinc oxide	5	5	5	5
Stearic acid	2	2	2	2
TMQ	1	1	1	1
6PPD	1.5	1.5	1.5	1.5
Antilux 654	2	2	2	2
Sulfur	1.5	1.5	1.5	1.5
CBS	0.75	0.75	0.75	0.75
Mnt	15	-	-	-
Mnt + 1.0 wt.% PPG	-	15	-	-
Mnt + 1.5 wt.% PPG	-	-	15	-
Mnt + 2.0 wt.% PPG	-	-	-	15

phr = parts per hundred parts of rubber.

Zhangjiagang, China) as follows: first, a mastication process for the reducing viscosity of the NR was implemented for 1.5 min. Second, SBR was added to the masticated NR and blended for 4.5 min. Third, other ingredients such as fillers, zinc oxide and so on were added and blended for 4.0 min. Finally, aromatic oil was added and blended for 5 min (master batch). Afterward, the rubber curatives were added to the master batch in a two-roll mill and blended for 5 min at 60°C. The compound formulation process is shown in Table 1.

Results and discussion

FTIR studies

The surface treatment of Mnt was considered using FTIR. The PPG spectrum (Fig. 1a) showed five characteristic bands assigned as 3312 cm⁻¹ for O–H stretching, 2941 and 2876 cm⁻¹ for C–H stretching, 1456 cm⁻¹ for C–H bending and 1085 cm⁻¹ for C–O stretching. Mnt presented five major bands (Fig. 1b). The band at 3625 cm⁻¹ was attributed to the O–H stretching bound to aluminium or magnesium of the Mnt (structural OH groups). The broad band at ~3389 cm⁻¹ and the band at 1636 cm⁻¹ corresponded to the O–H stretching of the adsorbed water and to the O–H bending of the intercalated water, respectively. The bands at 1004 and 915 cm⁻¹ corresponded to Si–O–Si and Si–OH stretching, respectively (Sarier & Onder, 2010; Songurtekin *et al.*, 2013; Bertuoli *et al.*, 2014). In the St-Mnt samples (Fig. 1c–e), especially St-Mnt with 1 wt.% PPG, there was an increase in the band intensity at ~1100 cm⁻¹, which corresponded to C–H stretching, and a band at ~2954 cm⁻¹, which corresponded to C–O stretching. These bands provided evidence of the grafting of PPG through shifting of the band at 1636 cm⁻¹ to a lower wavenumber (1633 cm⁻¹) due to the decrease in OH groups in St-Mnt (Sarier & Onder, 2010) and the absence of a band

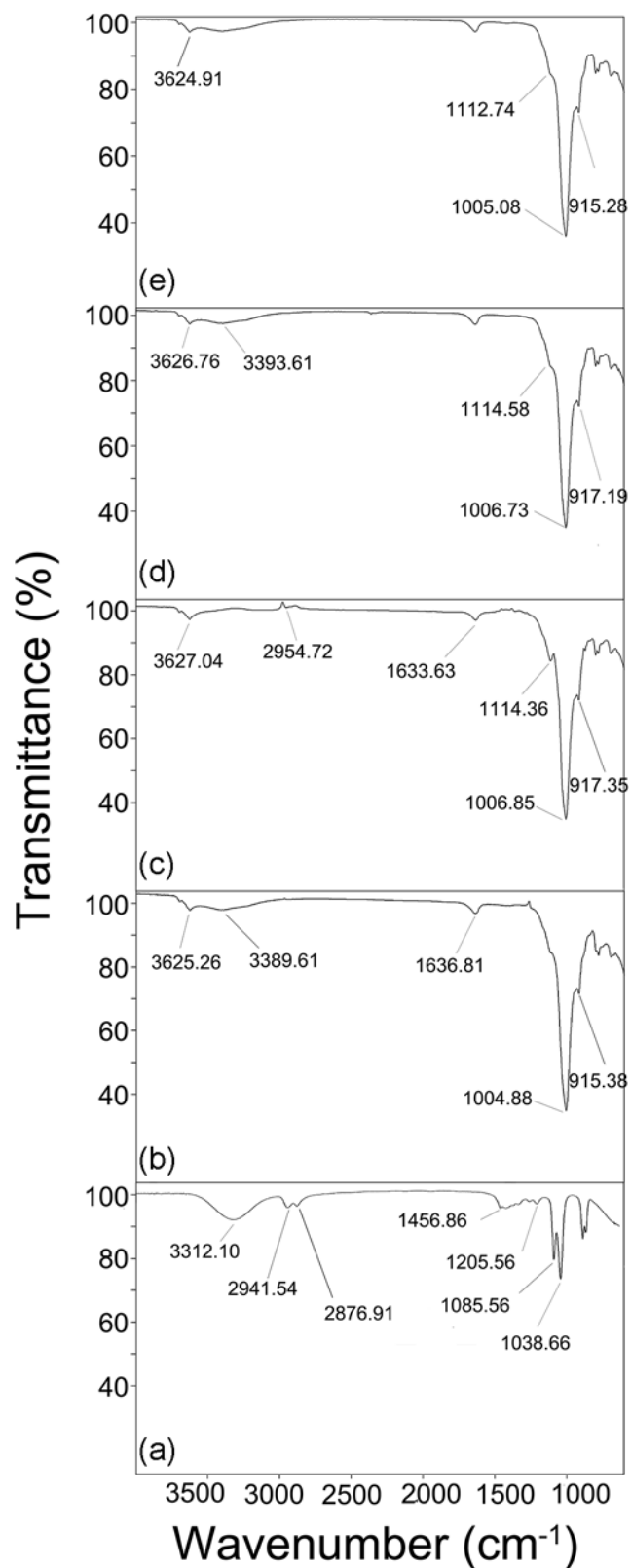


Figure 1. ATR-FTIR spectra of (a) PPG, (b) Mnt, (c) Mnt + 1.0 wt.% PPG, (d) Mnt + 1.5 wt.% PPG and (e) Mnt + 2.0 wt.% PPG.

at 3389 cm⁻¹ related to loss of adsorbed water, thereby verifying the surface treatment with PPG and decreased hydrophilicity of Mnt.

Thermal analysis studies

TGA was used to confirm the surface treatment of the Mnt. For PPG (Fig. 2a), the one-step decomposition was demonstrated and a mass loss of 99.87% up to 190°C was obtained. The TGA graph obtained from the Mnt sample (Fig. 2b) demonstrated the two-step decomposition that is typical of Mnt (Sarier & Onder, 2010; Songurtekin *et al.*, 2013; Belousov *et al.*, 2021). The first step took place between ambient temperature and 300°C due to the elimination of adsorbed water from the surface and interlayer space of Mnt. The rate of mass loss up to 190°C was rapid, leading to a mass loss of 8.21%. After that, up to ~300°C, the rate of mass loss reduced significantly, and it reached a value of 8.95%. The second step took place between 300°C and 850°C due to the dehydroxylation of the linked OH groups of the Mnt. A residual quantity of 84.65% was attained at 850°C. For the St-Mnt samples (Fig. 2c–e), a three-step decomposition was demonstrated. The first step took place between ambient temperature and 190°C. The mass losses in this temperature range of the St-Mnt samples with 1.0 wt.% PPG, 1.5 wt.% PPG and 2.0 wt.% PPG were 6.94%, 8.21% and 7.42%, respectively. The reduction of mass losses in this step, especially in the sample with 1.0 wt.% PPG, could imply a reduction of hydrophilic properties and an increase in hydrophobicity of Mnt (Zhou *et al.*, 2009). The second step occurred between 190°C and 350°C. The mass losses of the St-Mnt samples with 1.0 wt.% PPG, 1.5 wt.% PPG and 2.0 wt.% PPG were 3.15%, 1.04% and 0.65%, respectively. These reductions, especially for the St-Mnt with 1.0 wt.% PPG, can be explained by PPG degradation that intercalated within the interlayer space of Mnt. The third step occurred between 350°C and 850°C. The mass losses of the St-Mnt samples with 1.0 wt.% PPG, 1.5 wt.% PPG and 2.0 wt.% PPG were 5.13%, 4.97% and 4.84%, respectively. The residues of the St-Mnt samples with 1.0 wt.% PPG, 1.5 wt.% PPG and 2.0 wt.% PPG at 850°C were 84.78%, 85.78% and 87.09%, respectively.

SEM observations and energy-dispersive X-ray spectroscopy

SEM was applied to observe the morphology of Mnt and the St-Mnt samples. The shape and size of Mnt (Fig. 3a) showed overlapped layers that were tightly packed together and formed dense platelets. After surface treatment, the better-exfoliated state of the layers could be observed (Fig. 3b–d). This indicated the intercalation of PPG molecules in the interlayer spaces of Mnt, which resulted in increases in the interlayer spaces of the St-Mnt samples. The mass percentage of the elements that were detected using energy-dispersive X-ray spectroscopy (EDS) analyses are shown in Table 2. By comparing the structural elements of the samples, the difference between Mnt and the St-Mnt samples can be attributed to the presence of carbon in the St-Mnt samples. The presence of carbon in the St-Mnt samples could be due to the PPG grafted onto the Mnt, indicating that the surface treatment was successfully performed. It is worth noting that the highest level of carbon was obtained for the St-Mnt sample with 1.0 wt.% PPG.

XRD studies

XRD analysis was used to investigate the changes in the interlayer spaces of the Mnt after surface treatment by PPG. Mnt (Fig. 4a) showed two reflections at $1.68^{\circ}2\theta$ and $7.02^{\circ}2\theta$, which were assigned to the interlayer platelet spaces with spaces of 6.08 and 1.46 nm, respectively. The first reflection could be attributed to

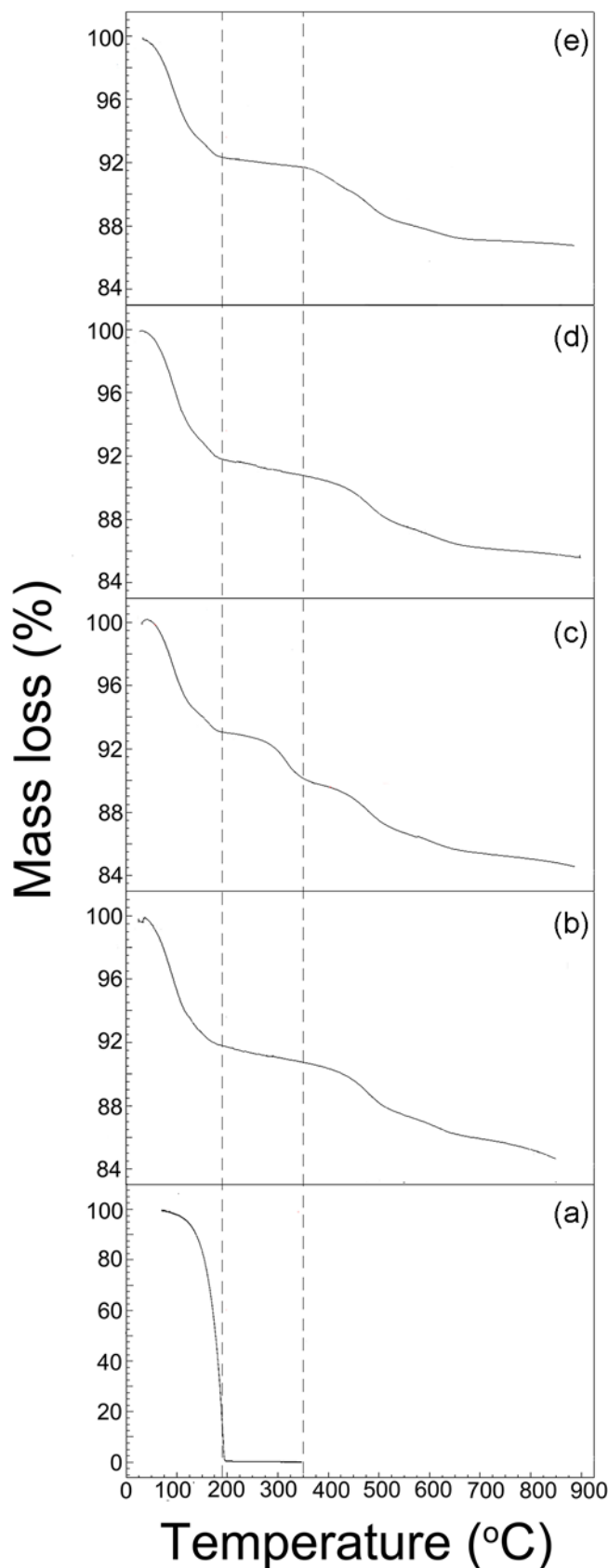


Figure 2. TGA curves: (a) PPG, (b) Mnt, (c) Mnt + 1.0 wt.% PPG, (d) Mnt + 1.5 wt.% PPG and (e) Mnt + 2.0 wt.% PPG.

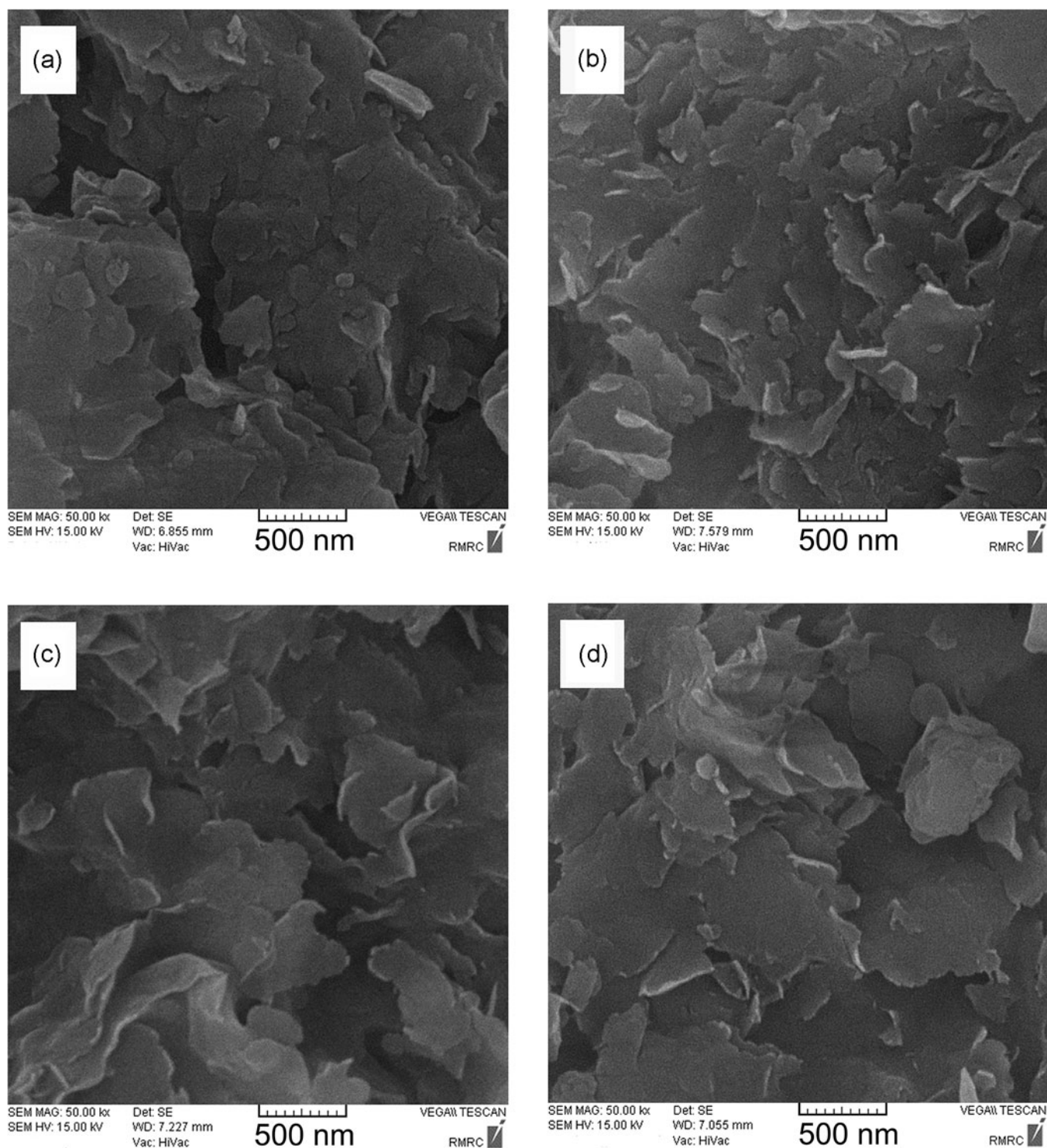


Figure 3. SEM images: (a) Mnt, (b) Mnt + 1.0 wt.% PPG, (c) Mnt + 1.5 wt.% PPG and (d) Mnt + 2.0 wt.% PPG.

the intercalation of impurities such as Fe cations into the Mnt interlayer spaces. The second reflection could be attributed to the (001) basal reflection of Mnt. In the St-Mnt samples (Fig. 4b–d), especially the St-Mnt sample with 1.0 wt.% PPG, an increase

in the interlayer space of Mnt was observed due to the intercalation of PPG molecules within the interlayer space of Mnt. Hence, shifting of Mnt reflections to lower 2θ values for the St-Mnt samples occurred (Zhou *et al.*, 2009; Songurtekin *et al.*, 2013;

Table 2. Mass percentages (wt.%) of the elements detected.

Element	Sample			
	Mnt	Mnt + 1.0 wt.% PPG	Mnt + 1.5 wt.% PPG	Mnt + 2.0 wt.% PPG
Au	10.87	9.95	7.36	4.03
Al	10.08	7.54	8.37	8.38
Si	22.01	17.96	19.08	19.48
Ca	0.71	0.77	1.00	1.55
Ti	0.25	0.08	0.23	0.29
K	0.82	0.51	0.83	1.03
Mg	1.18	0.70	0.94	0.86
O	51.34	49.72	51.20	54.30
C	-	10.19	7.87	6.51
Fe	2.75	2.57	3.13	3.58
Total	100.00	100.00	100.00	100.00

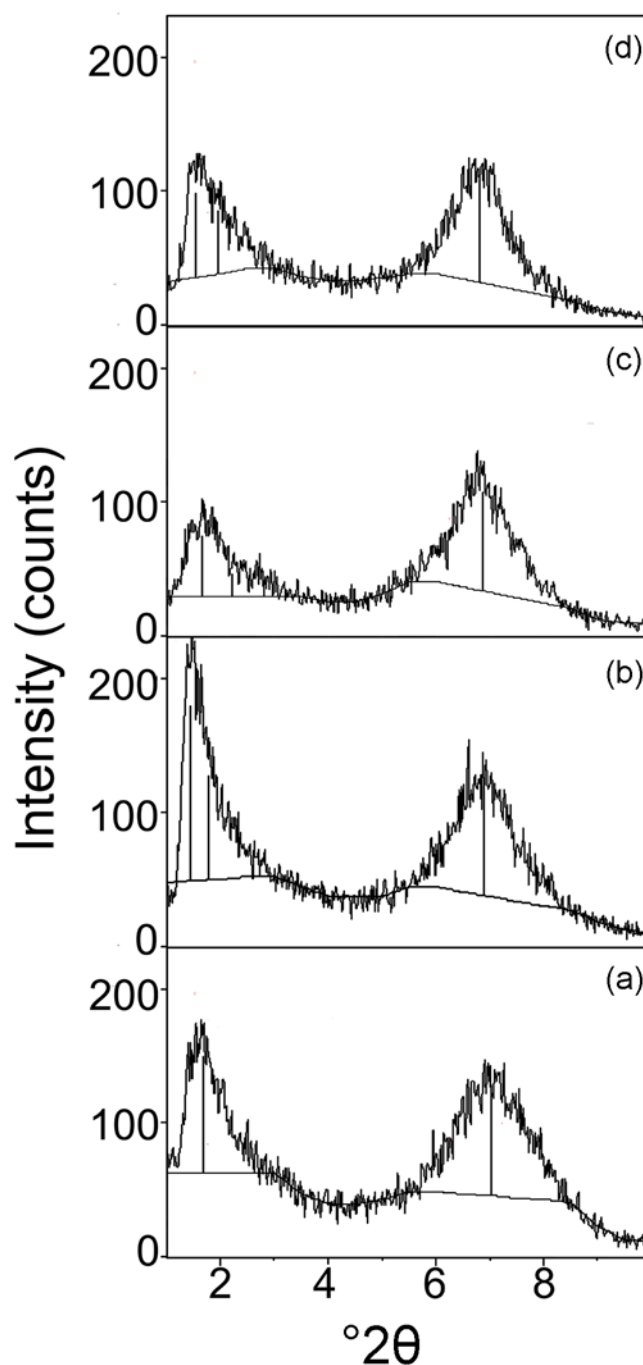
Bertuoli *et al.*, 2014). These changes confirmed the successful surface treatment of Mnt by PPG. These results are shown in Table 3.

Dispersion of the St-Mnt samples in the rubber matrix

Dispersions of the Mnt and St-Mnt samples in the rubber compounds were studied using SEM (Fig. 5). The bright grey features in the SEM images corresponded to the Mnt aggregates in the rubber compounds. The image obtained from the Mnt (Fig. 5a) revealed undesirable agglomeration and indicated the poor dispersibility of Mnt particles in the rubber matrix due to the incompatibility of hydrophilic Mnt with the hydrophobic matrix. After surface treatment by PPG, the SEM images (Fig. 5b–d) demonstrated the smoother structure of the rubber compounds. Mnt agglomerations were removed, and the dispersions of the St-Mnt samples in the rubber matrix were improved. This confirmed the reduction in hydrophilicity and increase in hydrophobicity of Mnt. The increase in hydrophobicity resulted in improved interfacial interactions between the rubber matrix and Mnt. In addition, increasing the interlayer spaces could facilitate the dispersion of Mnt in rubber compounds.

Table 3. XRD analysis results.

Sample	Position ($^{\circ}2\theta$)	<i>d</i> -value (nm)	Position ($^{\circ}2\theta$)	<i>d</i> -value (nm)
Mnt	1.68	6.08	7.02	1.46
Mnt + 1.0 wt.% PPG	1.45	7.04	6.89	1.49
	1.79	5.74	-	-
Mnt + 1.5 wt.% PPG	1.67	6.13	6.88	1.49
	2.21	4.63	-	-
Mnt + 2.0 wt.% PPG	1.55	6.62	6.80	1.51
	1.96	5.22	-	-

**Figure 4.** XRD traces: (a) Mnt, (b) Mnt + 1.0 wt.% PPG, (c) Mnt + 1.5 wt.% PPG and (d) Mnt + 2.0 wt.% PPG.

Cure characteristics

The cure characteristics of the rubber compounds are shown in Table 4.

Scorch time

The St-Mnt samples filled rubber compounds, especially the St-Mnt with 1 wt.% PPG, as illustrated by the shorter scorch time (T_{s2}) values as compared to the Mnt-filled rubber compound. The

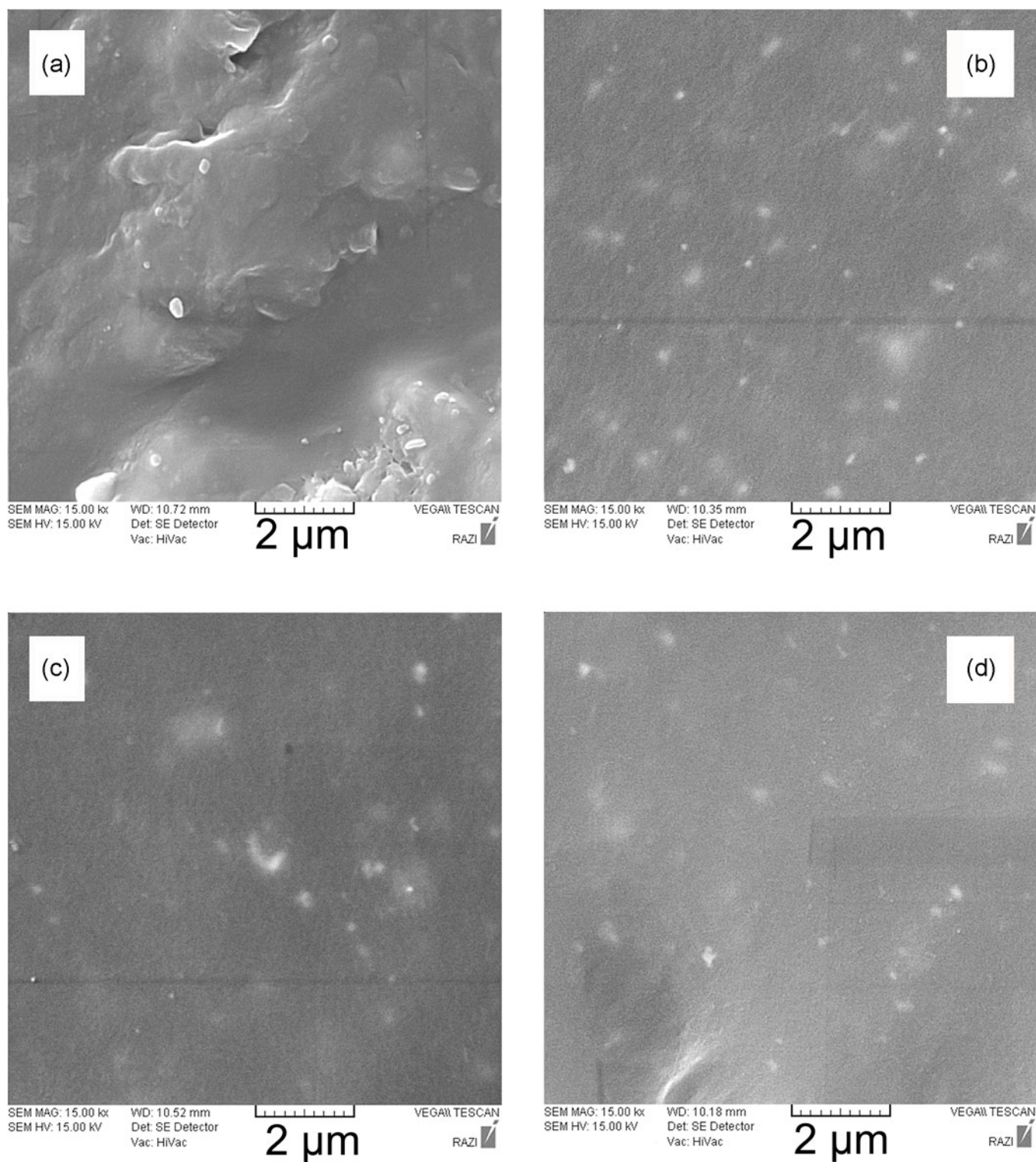


Figure 5. SEM images of the rubber compounds based on NR/SBR filled with Mnt and St-Mnt samples: (a) Mnt, (b) Mnt + 1.0 wt.% PPG, (c) Mnt + 1.5 wt.% PPG and (d) Mnt + 2.0 wt.% PPG.

shorter T_{S_2} values may be due to the exfoliated structure and uniform dispersion of St-Mnt in the rubber matrix, which could accelerate the heat transfer, facilitating the formation of cross-linkages during the cure process and speeding up the cure process.

Optimum cure time

The results showed that the optimum cure time ($T_{C_{90}}$) values of the rubber compounds decreased with the addition of St-Mnt samples, and the shortest value was obtained when using the St-Mnt sample

Table 4. Rubber compound properties.

Property	Compound			
	1 Mnt	2 Mnt + 1.0 wt.% PPG	3 Mnt + 1.5 wt.% PPG	4 Mnt + 2.0 wt.% PPG
T _{S2} (s)	369.60	331.12	361.20	366.60
T _{C90} (s)	754.80	628.20	699.60	689.40
CRI (min ⁻¹)	14.90	20.34	19.14	17.74
M _L (dNm)	0.69	0.83	0.83	0.97
M _H (dNm)	4.69	5.10	5.10	5.24
M _H - M _L (dNm)	4	4.28	4.28	4.27
Abrasion loss (mm ³)	536	307	423	406
Resilience (%)	47.67	49.60	48.52	46.60
Compression set (%)	39.13	37.68	36.84	37.14
Ozone resistance	No cracks	No cracks	No cracks	No cracks

with 1.0 wt.% PPG. After surface treatment, the rubber–filler interaction could be improved due to the increased hydrophobicity of Mnt. Accordingly, a uniform dispersion of St-Mnt particles in the non-polar rubber matrix was obtained, which resulted in superior heat transfer through the curing process. Reducing the curing time has a significant effect on lowering energy consumption and operation costs, which is highly valuable.

Cure rate index

The cure rate index (CRI) as an indicator of the curing reaction speed was increased when using treated samples, confirming the more rapid curing system for the rubber compounds filled with St-Mnt samples, especially for the sample treated with 1.0 wt.% PPG.

Torque difference ($M_H - M_L$)

The torque difference ($M_H - M_L$) value is an indicator of the amount of pure cross-link density. It was increased when using the St-Mnt samples as fillers. The greater $M_H - M_L$ values in the compounds containing the St-Mnt samples confirmed the greater cross-link densities, which were associated with increased hardness values due to the improved filler dispersion.

Mechanical properties

The mechanical properties (abrasion resistance, resilience, compression set and ozone resistance) of the compounds are reported in Table 4.

Abrasion resistances

Abrasion losses were decreased when using the St-Mnt samples; thus, abrasion resistances could be increased with surface treatment. The improved abrasion resistances for the compounds

containing the treated samples, especially for St-Mnt with 1.0 wt.% PPG, are indicated by the greater hardness values and improved dispersions of the St-Mnt samples in the rubber compounds.

Resilience

The resilience value for the rubber compound with 1.0 wt.% of PPG was increased, confirming the improvement with surface treatment. PPG has a plasticizing effect that could maintain the elasticity of the rubber chains along with increasing the rubber reinforcement.

Compression set

The compression set values were decreased when applying the St-Mnt samples. The improved interfacial interaction of the rubber matrix with the St-Mnt samples as fillers resulted in improved reinforcing effects with the St-Mnt samples in comparison with Mnt, and decrease the compression set of the rubber compounds.

Ozone resistance

No cracks were observed for all of the samples, which confirmed the good ozone resistance of the compounds.

Thermal properties of the rubber compounds

The curves obtained from the TGA and differential thermogravimetric (DTG) analysis of the rubber compounds (Figs 6 & 7) showed a three-step decomposition (i.e. the same as a typical TGA of rubber compounds) corresponding to volatilization of moisture and those additives with lower boiling points such as oil and plasticizers, thermal degradation of rubber chains and carbon black combustion when the nitrogen atmosphere was changed to an air atmosphere. Mineral additives such as inorganic fillers and ZnO remain as the residue (ash content; Gupta *et al.*, 2013). In the second step (main decomposition), the temperatures of initial decomposition and final decomposition and the temperature at the maximum rate of degradation (T_p) were considered to investigate the thermal stability of the products (Table 5). In the rubber compounds filled with St-Mnt samples, significant decreases in the initial decomposition temperature could be observed, showing that the thermal degradation of rubber compounds filled with St-Mnt samples started at lower temperatures. Furthermore, the interval between the initial and final temperatures of decomposition for St-Mnt filled compounds was increased, therefore indicating that the rate of degradation in the St-Mnt filled compounds was decreased. The decrease in initial decomposition temperature of the St-Mnt filled compounds might be due to the degradation of PPG at that temperature, and hence the St-Mnt filled compounds started to degrade at lower temperatures. The degradation of PPG as a treatment agent with an organic nature could provide catalytic effects by creating Lewis acids at the Mnt edges. By contrast, the barrier properties that were obtained *via* the homogeneous dispersion of St-Mnt samples as fillers in the rubber matrix increased the interval between the initial and final temperatures of decomposition, which could counterbalance the catalytic effects of the St-Mnt samples and result in improved thermal properties (Carli *et al.*, 2011).

As a general trend, after surface treatment, exfoliation of Mnt and the interlayer space between the plates increased; in addition, the hydrophobic properties of the Mnt increased. Therefore, interfacial interactions between the filler and the rubber were improved, and particles of filler became more compatible with

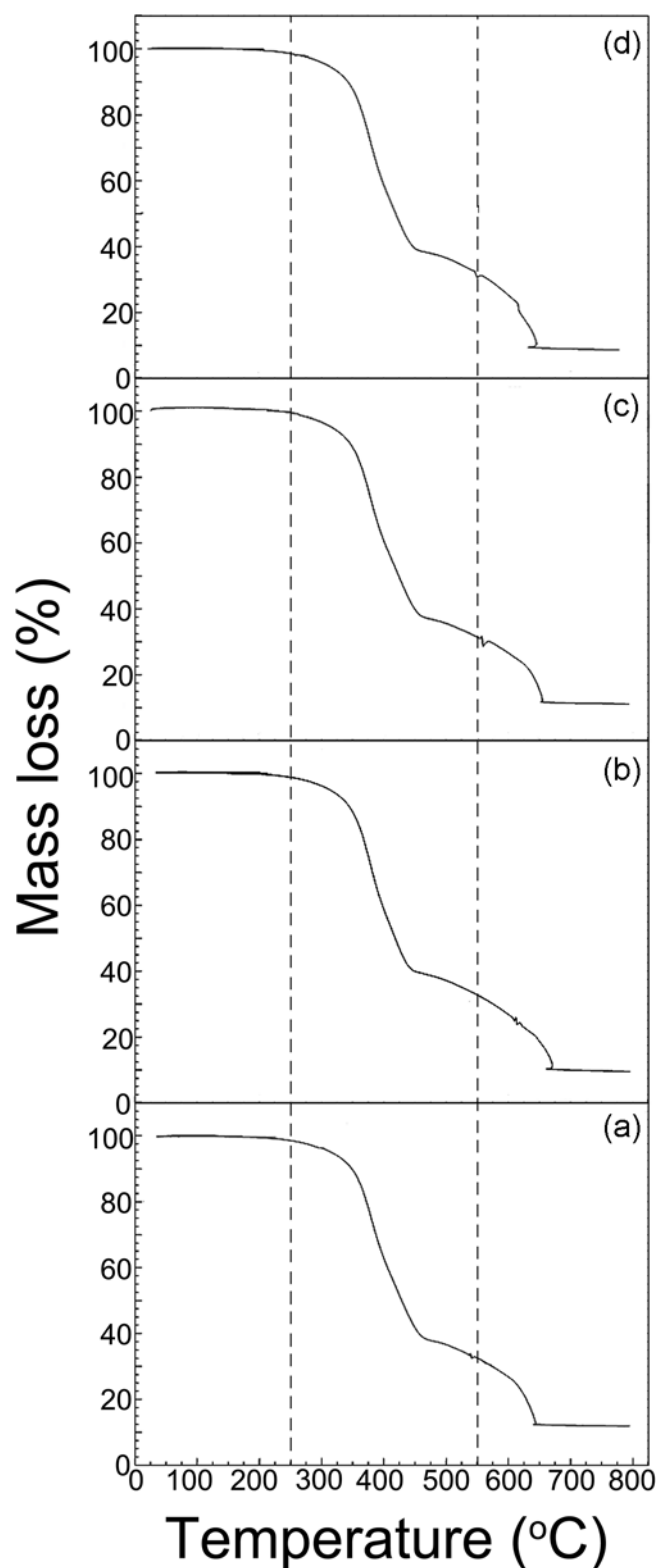


Figure 6. TGA curves of the rubber compounds: (a) Mnt, (b) Mnt + 1.0 wt.% PPG, (c) Mnt + 1.5 wt.% PPG and (d) Mnt + 2.0 wt.% PPG.

the hydrophobic rubber matrix; thus, improved reinforcing effects of the St-Mnt samples were observed compared to that of the untreated Mnt.

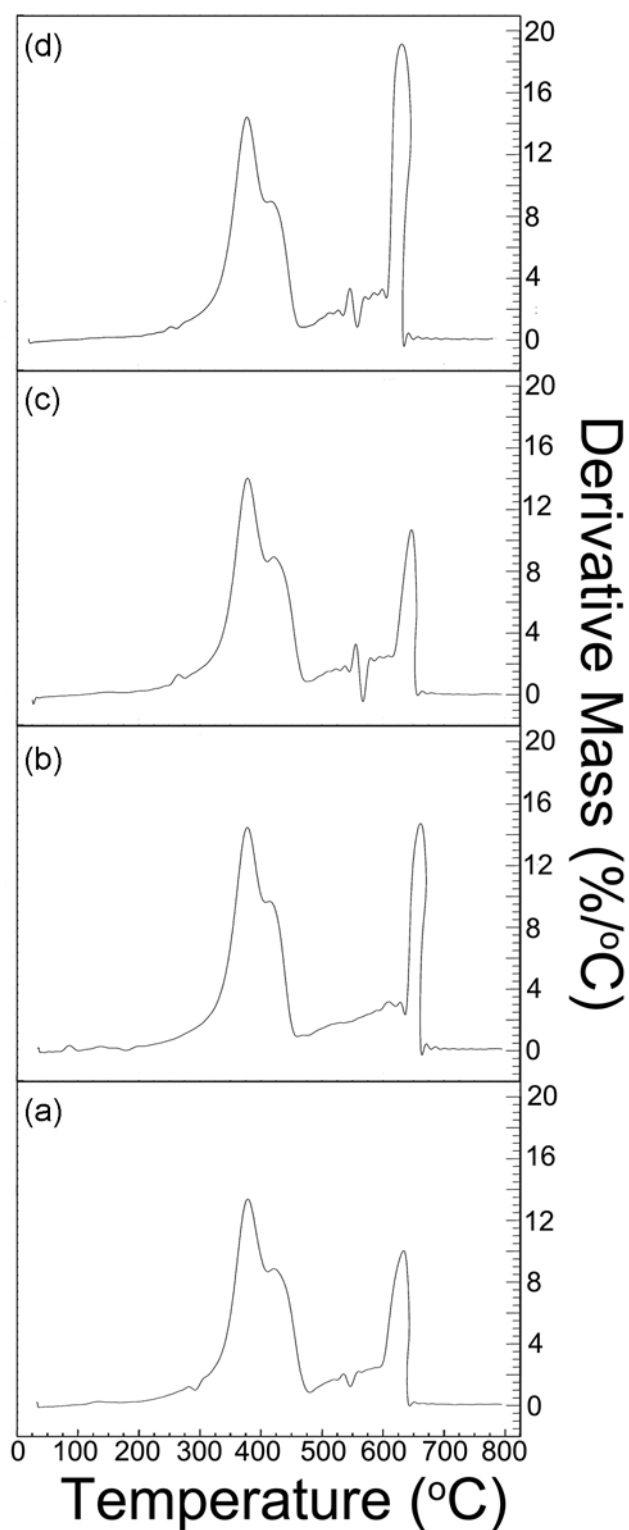


Figure 7. DTG curves of the rubber compounds: (a) Mnt, (b) Mnt + 1.0 wt.% PPG, (c) Mnt + 1.5 wt.% PPG and (d) Mnt + 2.0 wt.% PPG.

Conclusions

A new approach to the surface treatment of Mnt using various dosages of PPG has been assessed for its potential in the utilization of Mnt as a filler in non-polar rubber compounds. The results confirmed the successful surface treatment due to the more exfoliated

Table 5. TGA and DTG results for the rubber compounds.

Compound	Second step (main decomposition)			
	T_{initial} (°C)	T_{final} (°C)	T_{p1} (°C)	T_{p2} (°C)
Mnt	293	543	378	423
Mnt + 1.0 wt.% PPG	264	545	379	417
Mnt + 1.5 wt.% PPG	277	542	379	423
Mnt + 2.0 wt.% PPG	267	546	378	420

structure and increased interlayer space of the St-Mnt particles. The St-Mnt/carbon black-filled rubber compounds had shorter T_{S_2} and $T_{\text{C}_{90}}$ values along with increased CRI values. These results lead to reduced cure costs during the curing process due to the decreased processing time. The $M_{\text{H}} - M_{\text{L}}$ values for the rubber compounds filled with St-Mnt samples were increased, meaning that more reinforced compounds were formed. The mechanical properties of the rubber compounds, including abrasion resistance, resilience and compression set, all improved after surface treatment of the Mnt particles. The thermal study of the compounds indicated that the interval between the initial and final temperatures of decomposition increased after surface treatment of the Mnt particles. This treatment improved the rubber–filler interaction through increasing the hydrophobicity of the Mnt surface, resulting in a more uniform and improved dispersion of the filler particles within the rubber matrix without agglomeration. Heat transfer was facilitated under these conditions, and the cure process became more efficient. By comparing the obtained results, the St-Mnt with 1 wt.% PPG provided the best overall outcomes in terms of the curing system, mechanical properties and thermal stability of the rubber compound. These results provide new avenues for using St-Mnt as an environmentally friendly filler in the rubber industry to improve the properties of rubber goods, especially green tyres. Future work could focus on increasing the degree of dispersion and improving the compatibility of Mnt with non-polar rubber compounds by using a dual surface treatment system containing PPG and a coupling agent that is suitable for combination with PPG.

Acknowledgements. The authors thank the Iran Rubber Research Institute for its support of this experimental work.

Competing interests. The authors declare none.

References

Ahmadi F., Ghanbari H., Shabani Moghaddam F. & Naghizadeh R. (2022) Optimized purification procedure for Iranian calcium bentonite for producing montmorillonite nanosheets. *Clay Minerals*, **57**, 120–130.

Al-Shemmari F.H.J., Rabah A.A., Al-Mulla E.A.J. & Alrahman N.O.M.A. (2013) Preparation and characterization of natural rubber latex/modified montmorillonite clay nano-composite. *Research on Chemical Intermediates*, **39**, 4293–4301.

Alwis G.M.C., Kottegoda N. & Ratnayake U.N. (2020) Facile exfoliation method for improving interfacial compatibility in montmorillonite-natural rubber nanocomposites: a novel charge inversion approach. *Applied Clay Science*, **191**, 105633.

Antosik A.K., Mozelewska K., Musik M., Miadlicki P., Srensek-Nazzal J. & Wilpizewska K. (2023) The effect of neat and modified montmorillonite on thermal properties of silicone pressure-sensitive adhesives. *International Journal of Adhesion and Adhesives*, **130**, 103609.

Arabmofrad S., Jafari S.M., Lazzara G., Ziaifard A.M., Shahiri Tabarestani H., Bahlakeh G. et al. (2023) Preparation and characterization of surface-modified montmorillonite by cationic surfactants for adsorption purposes. *Journal of Thermal Analysis and Calorimetry*, **148**, 13803–13814.

Archibong F.N., Orakwe L.C., Ogah O.A., Mbam S.O., Ajah S.A., Okechukwu M.E. et al. (2023) Emerging progress in montmorillonite rubber/polymer nanocomposites: a review. *Journal of Materials Science*, **58**, 2396–2429.

Arroyo M., López-Manchado M.A. & Herrero B. (2003) Organomontmorillonite as substitute of carbon black in natural rubber compounds. *Polymer*, **44**, 2447–2453.

Baghitabar K., Jamshidi M. & Ghamarpoor R. (2023) Exfoliation, hydroxylation and silanization of two-dimensional (2D) montmorillonites (MMTs) and evaluation of the effects on tire rubber properties. *Polymer Testing*, **129**, 108265.

Belousov P., Chupalenkov N., Christidis G.E., Zakusina O., Zakusin S., Zakusin S. et al. (2021) Carboniferous bentonites from 10Th Khutor deposit (Russia): Composition, properties and features of genesis. *Applied Clay Science*, **215**, 106308.

Bertuoli P.T., Piazza D., Scienza L.C. & Zattera A.J. (2014) Preparation and characterization of montmorillonite Modified with 3-aminopropyltriethoxysilane. *Applied Clay Science*, **87**, 46–51.

Carli L.N., Crespo J.S. & Mauler R.S. (2011) PHBV nanocomposites based on organomodified montmorillonite and halloysite: the effect of clay type on the morphology and thermal and mechanical properties. *Composites: Part A*, **42**, 1601–1608.

Chen Y., Sun K., Zhang T., Zhou J., Liu Y., Zeng M. et al. (2023) TiO₂-modified montmorillonite-supported porous carbon-immobilized Pd species nanocomposite as an efficient catalyst for Sonogashira reactions. *Molecules*, **28**, 2399.

Chrissafis K. & Bikiaris D. (2011) Can nanoparticles really enhance thermal stability of polymers? Part I: an overview on thermal decomposition of addition polymers. *Thermochimica Acta*, **523**, 1–24.

Christidis G.E., Chryssikos G.D., Derkowski A., Dohrmann R., Eberl D.D., Joussein E. et al. (2023) Methods for determination of the layer charge of smectites: a critical assessment of existing approaches. *Clays and Clay Minerals*, **71**, 25–53.

Das A., Stockelhuber K.W., Jurk R., Jehnichen D. & Heinrich G. (2011) A general approach to rubber–montmorillonite nanocomposites: intercalation of stearic acid. *Applied Clay Science*, **51**, 117–125.

Esmaeili E., Rounaghi S.M. & Eckert J. (2021) Mechanochemical synthesis of rosin-modified montmorillonite: a breakthrough approach to the next generation of OMMT/rubber nanocomposites. *Nanomaterials*, **11**, 1974–1987.

Fathurrohman M.I., Rugmai S., Hayemasae N. & Sahakaro K. (2020) Better balance of silica-reinforced natural rubber tire tread compound properties by the use of montmorillonite with optimum surface modifier content. *Rubber Chemistry and Technology*, **93**, 548–566.

Gua Y.X., Liu J.H., Gates W.P. & Zhou C.H. (2020) Organo-modification of montmorillonite. *Clay and Clay Minerals*, **68**, 601–622.

Gupta S.D., Mukhopadhyay R., Baranwal K.C. & Bhowmick A.K. (2013) *Reverse Engineering of Rubber Products: Concepts, Tools, and Techniques*. CRC Press, Boca Raton, FL, USA, 357 pp.

Jincheng W., Youcheng D., Kai S., Yibo S., Chen P. & Yi Z. (2013) Organoclays prepared from montmorillonites with tetramethylphosphonium chloride in different pH conditions. *Powder Technology*, **247**, 178–187.

Kazemi H., Mighri F. & Rodrigue D. (2022) A review of rubber biocomposites reinforced with lignocellulosic fillers. *Journal of Composites Science*, **6**, 183–214.

Kovalchuk I. (2023) Performance of thermal-, acid-, and mechanochemical-activated montmorillonite for environmental protection from radionuclides U(VI) and Sr(II). *Eng – Advances in Engineering*, **4**, 2141–2152.

Krol-Morkisz K. & Pielichowska K. (2018) Thermal decomposition of polymer nanocomposites with functionalized nanoparticles. Pp. 405–435 in: *Polymer Composites with Functionalized Nanoparticles*. (K. Pielichowski & T.M. Majka, editors). Elsevier, Amsterdam, The Netherlands.

Krzaczowska J., Fojud Z., Kozak M. & Jurga S. (2005) Spectroscopic studies of poly(ϵ -caprolactone)/sodium montmorillonite nanocomposites. *Acta Physica Polonica A*, **108**, 187–196.

- Lan D.N.U., Bakar A.A., Azahari B., Ariff Z.M. & Chujo Y. (2012) Effect of interlocking between porous microparticles and elastomer on mechanical properties and deformation modes. *Polymer Testing*, **31**, 931–937.
- Liu X., Zhou F., Chi R., Feng J., Ding Y. & Liu Q. (2019) Preparation of modified montmorillonite and its application to rare earth adsorption. *Minerals*, **9**, 747–760.
- Madejova J., Barlog M., Slany M., Bashir S., Scholtzova E., Tunega D. et al. (2023) Advanced materials based on montmorillonite modified with poly(ethylenimine) and poly(2-methyl-2-oxazoline): Experimental and DFT study. *Colloids and Surfaces A: Physicochemical and Engineering Aspects*, **659**, 130784.
- Meng Z., Li J., Zou Y., Li N., Fu X., Zhang R. et al. (2022) Advanced montmorillonite modification by using corrosive microorganisms as an alternative filler to reinforce natural rubber. *Applied Clay Science*, **225**, 106534.
- Miedzianowska J., Maslowski M., Rybínski P. & Strzelec K. (2021) Modified nanoclays/straw fillers as functional additives of natural rubber biocomposites. *Polymers*, **13**, 799–828.
- Mohamed R.M. (2013) Radiation induced modification of NBR and SBR montmorillonite nanocomposites. *Journal of Industrial and Engineering Chemistry*, **19**, 80–86.
- Moonchai D., Moryadee N. & Poosodsang N. (2012) Comparative properties of natural rubber vulcanisates filled with defatted rice bran, clay and calcium carbonate. *Maejo International Journal of Science and Technology*, **6**, 249–258.
- Moustafa H., Lawandy S.N., Rabee M. & Zahran M.A.H. (2020) Effect of green modification of nanoclay on the adhesion behavior of EPDM rubber to polyester fabric. *International Journal of Adhesion and Adhesives*, **100**, 102617.
- Olszewski A., Lawniczak A., Kosmela P., Strakowski M., Mielewczyk-Gryn A., Hejna A. et al. (2023) Influence of surface-modified montmorillonite clays on the properties of elastomeric thin layer nanocomposites. *Materials*, **16**, 1703.
- Pajtašová M., Mičicová Z., Ondrušová D., Pecušová B., Feriancová A., Raník L. et al. (2017) Study of properties of fillers based on natural bentonite and their effect on the rubber compounds. *Procedia Engineering*, **177**, 470–475.
- Pattamaprom C. & Jiamjitsiripong K. (2012) Effects of layered silicate fillers and their surface treatments in NR/BIIR blend. *International Transaction Journal of Engineering, Management, & Applied Sciences & Technologies*, **3**, 381–399.
- Rath J.P., Chaki T.K. & Khastgir D. (2012) Development of natural rubber-fibrous nano clay attapulgite composites: the effect of chemical treatment of filler on mechanical and dynamic mechanical properties of composites. *Procedia Chemistry*, **4**, 131–137.
- Safarik I. & Prochazkova J. (2024) Soil montmorillonite can exhibit peroxidase-like activity. *Clay Minerals*, **59**, 22–25.
- Sarier N. & Onder E. (2010) Organic modification of montmorillonite with low molecular weight polyethylene glycols and its use in polyurethane nanocomposite foams. *Thermochimica Acta*, **510**, 113–121.
- Sarma A.D., Federico C.E., Nzulu F., Weydert M., Verge P. & Schmidt D.F. (2021) Multipurpose processing additives for silica/rubber composites: synthesis, characterization, and application. *Polymers*, **13**, 3608–3621.
- Seo J.G., Lee C.K., Lee D. & Song S.H. (2018) High-performance tires based on graphene coated with Zn-free coupling agents. *Journal of Industrial and Engineering Chemistry*, **66**, 78–85.
- Shuai C., Yu L., Feng P., Zhong Y., Zhao Z., Chen Z. et al. (2020) Organic montmorillonite produced an interlayer locking effect in a polymer scaffold to enhance interfacial bonding. *Materials Chemistry Frontiers*, **4**, 2398–2408.
- Song K. & Sandi G. (2001) Characterization of montmorillonite surfaces after modification by organosilane. *Clays and Clay Minerals*, **49**, 119–125.
- Songurtekin D., Yalcinkaya E.E., Ag D., Selici M., Demirkol D.O. & Timur S. (2013) Histidine modified montmorillonite: laccase immobilization and application to flow injection analysis of phenols. *Applied Clay Science*, **86**, 64–69.
- Su H., Zhang Y., Zhou J. & Hou Q. (2023) Molecular dynamics simulation of dodecyl dimethyl benzyl ammonium cation-intercalated montmorillonite. *Clay Minerals*, **58**, 415–423.
- Utrera-Barrios S., Perera R., León N., HernándezSantana M. & Martínez N. (2021) Reinforcement of natural rubber using a novel combination of conventional and in situ generated fillers. *Composites Part C*, **5**, 100133.
- Wang L., Fu W., Peng W., Xiao H., Li S., Huang J. et al. (2019) Enhancing mechanical and thermal properties of polyurethane rubber reinforced with polyethylene glycol-g-graphene oxide. *Advances in Polymer Technology*, **2019**, 2318347.
- Wójcik-Bania M. & Matusik J. (2021) The effect of surfactant-modified montmorillonite on the cross-linking efficiency of polysiloxanes. *Materials*, **14**, 2623–2638.
- Xi Y., Frost R.L. & He H. (2007) Modification of the surfaces of Wyoming montmorillonite by the cationic surfactants alkyl trimethyl, dialkyl dimethyl, and trialkyl methyl ammonium bromides. *Journal of Colloid and Interface Science*, **305**, 150–158.
- Yotsuji K., Tachi Y., Sakuma H. & Kawamura K. (2021) Effect of interlayer cations on montmorillonite swelling: comparison between molecular dynamic simulations and experiments. *Applied Clay Science*, **204**, 106034.
- Yu W.H., Liu J.H., Wang M., Li N., Zhang J.R., Huang T.H. et al. (2021) Dispersion and swellability of ternary surfactant co-modified montmorillonites. *Clays and Clay Minerals*, **69**, 759–771.
- Zhang H., Xing W., Li H., Xie Z., Huang G. & Wu J. (2019) Fundamental researches on graphene/rubber nanocomposites. *Advanced Industrial and Engineering Polymer Research*, **2**, 32–41.
- Zhang Q., Liu, Q., Zhang Y., Cheng H. & Lu Y. (2012) Silane-grafted silica-covered kaolinite as filler of styrene butadiene rubber. *Applied Clay Science*, **65–66**, 134–138.
- Zhou L., Chen H., Jiang X., Lu F., Zhou Y., Yin W. et al. (2009) Modification of montmorillonite surfaces using a novel class of cationic Gemini surfactants. *Journal of Colloid and Interface Science*, **332**, 16–21.
- Zhou S.Q., Niu Y.Q., Liu J.H., Chen X.X., Li C.S., Gates W.P. & Zhou C.H. (2022) Functional montmorillonite/polymer coatings. *Clays and Clay Minerals*, **70**, 209–232.